Hindawi Publishing Corporation
ISRN Biomaterials
Volume 2013, Article ID 649163, 11 pages
http://dx.doi.org/10.5402/2013/649163

Research Article

Strontium Incorporated Coralline Hydroxyapatite for Engineering Bone

Waiching Liu,[1] Ting Wang,[1] Yuhui Shen,[2] Haobo Pan,[1,3] Songlin Peng,[1,4] and William W. Lu[1,3]

[1] *Department of Orthopaedics & Traumatology, The University of Hong Kong, Pokfulam, Hong Kong*
[2] *Department of Orthopaedics, Shanghai Institute of Orthopaedics & Traumatology, Shanghai Ruijin Hospital, Shanghai Jiao Tong University School of Medicine, 227 South Chongqing Road, Shanghai 20025, China*
[3] *Center for Human Tissues and Organs Degeneration, Shenzhen Institute of Advanced Technology, Chinese Academy of Science, 1068 Xueyuan Avenue, Shenzhen University Town, Shenzhen 518055, China*
[4] *Department of Spine Surgery, Shenzhen People's Hospital, Jinan University Second College of Medicine, 1017 Dong Min Bei Lu, Shenzhen 518020, China*

Correspondence should be addressed to Haobo Pan; haobo@hku.hk, and William W. Lu; wwlu@hku.hk

Received 9 October 2012; Accepted 24 October 2012

Academic Editors: S. Lamponi, J. Wang, and X. Wang

Goniopora was hydrothermally converted to coralline hydroxyapatite (CHA) and incorporated with Sr (Sr-CHA). The pore size of Goniopora was in the range of 40–300 μm with a porosity of about 68%. Surface morphologies of the coral were modified to flake-like hydroxyapatite structures on CHA and the addition of Sr detected on Sr-CHA as confirmed by SEM and EDX. As the first report of incorporating Sr into coral, about 6%–14% Sr was detected on Sr-CHA. The compressive strengths of CHA and Sr-CHA were not compromised due to the hydrothermal treatments. Sr-CHA was studied *in vitro* using MC3T3-E1 cells and *in vivo* with an ovariectomized rat model. The proliferation of MC3T3-E1 cells was significantly promoted by Sr-CHA as compared to CHA. Moreover, higher scaffold volume retention (+40%) was reported on the micro-CT analysis of the Sr-CHA scaffold. The results suggest that the incorporation of Sr in CHA can further enhance the osteoconductivity and osteoinductivity of corals. Strontium has been suggested to stimulate bone growth and inhibit bone resorption. In this study, we have successfully incorporated Sr into CHA with the natural porous structure remained and explored the idea of Sr-CHA as a potential scaffolding material for bone regeneration.

1. Introduction

Reconstruction of massive bone defects caused by severe traumas and tumors remains a great challenge in orthopaedics. The preferred treatment is autologous bone graft, but the supply is usually limited due to the mobility and pain caused to the patient [1, 2]. Immunological response of our body and possibility of contamination have limited the use of allograft. Emergence of tissue engineering has been growing promisingly in orthopaedics as an alternative approach for bone regeneration. Before supplementing scaffolds with marrow stromal cells and growth factors to further enhance bone regeneration, the choices of scaffold with osteoconductivity or even osteoinductivity are important to start with.

Coral, which usually refers to the exoskeleton of natural coral, has been a material of interest in orthopaedic biomaterial due to its chemical composition and structural and mechanical properties. Other materials have to be further modified to meet the essential structural, physical, or mechanical requirements of ideal bone substitutes; however, natural coral, primarily reef-building coral, has certain degrees of similarity to human bone without the need of modification [3]. Major component of coral is calcium carbonate (97–99%), in aragonite form, with 1–1.5% of organic substances and little trace elements (0.5–1% of magnesium, sodium, potassium, strontium, fluorine, phosphorous, etc.) [3–5].

Since Roy and Linnehan first published in 1974, hydrothermal reaction has been widely applied to convert

natural coral from calcium carbonate to calcium hydroxyapatite, also known as coralline hydroxyapatite (CHA), by keeping the porous microstructure of coral [6]. Both natural coral and CHA have their own advantages and drawbacks; while the decision is predominantly based on the different weighting on the mechanical property and biodegradability and compositional similarity to bone [3]. More importantly, natural coral and CHA can supply plenty of calcium and possess micropores with interconnectivity, which are helpful in bone regeneration and essential for bone ingrowth in terms of tissue engineering scaffold [4, 7–9].

Strontium has been well published for its antiresorptive and anabolic effects on bone, so it is gaining attention on its applications in orthopaedic biomaterials [10]. It is believed that the addition of Sr can modify or further enhance the bioactivity of materials, particularly for the materials to be applied in osteoporotic and osteopenic patients. In this study, Sr was incorporated to CHA converted from Goniopora as a new scaffolding material for bone tissue engineering; Goniopora has been one of the few genera of corals, in which it has been widely studied in the literature for biomedical applications. The mechanical properties, chemical composition, and morphological changes were characterized; the biological properties were investigated *in vitro* and *in vivo* with an OVX rat model.

2. Materials and Methods

2.1. Hydrothermal Conversion and Incorporation of Strontium. Coralline hydroxyapatite (CHA) conversion was based on the calcium available in the coral reacted with diammonium hydrogen phosphate converting it into hydroxyapatite. Goniopora was obtained from the South China Sea near Sanya, China. Once received, it was immersed in 5% sodium hypochlorite solution and rinsed with distilled water several times until all the proteins were removed as widely reported [3]. The molar ratio of $CaCO_3$ to $(NH_4)_2HPO_4$ is 10 : 6 in order to prepare 1 mole of $Ca_{10}(PO_4)_6(OH)_2$ [6]. Coral specimens were filled with 2 M diammonium hydrogen phosphate (pH 8.0) solution in excess (5 times of the required amount) and put in a hydrothermal bomb [11]. The bomb was set in a 180°C oven for 15 h and replaced with fresh $(NH_4)_2HPO_4$ solution to being further treated for 15 h as a 2-day treatment. Strontium was hydrothermally incorporated into CHA (i.e., Sr-CHA) by adding strontium nitrate (0.1 M or 0.5 M) solutions for 15 h at 180°C; the molar ratios of Sr to Ca for 0.1 M $Sr(NO_3)_2$ and 0.5 M $Sr(NO_3)_2$ solutions were Sr : Ca = 4 : 10 and 12 : 10, respectively. All chemicals used were purchased from Sigma-Aldrich (St. Louis, MO, USA) and Wako Pure Chemical Industries (Japan) unless specified.

2.2. Structural Evaluation and Compressive Properties. The microstructure and compressive properties of specimens were studied by micro-CT and compression test. Raw Goniopora was scanned using SkyScan 1076 (Kontich, Belgium) micro-CT scanner with the pixel size set to 11.53 μm. Three-dimensional model and porosity measurement were performed using SkyScan CTAn software. Compression test was performed on the specimens cut in the size of $6 \times 6 \times 8\,mm^3$. Testing was undergone on the 6 × 6 mm surface along the height of 8 mm with a recording material testing machine (MTS 858 Bionix machine, MTS System, Minneapolis, MN, USA) with the compression rate of 2 mm/min. Five specimens each of the untreated coral, CHA, and Sr-CHA were taken for the compression test.

2.3. Characterization. Degree of conversion, percentage of Sr substitution, and surface morphology of CHA and Sr-CHA scaffolds were studied with SEM, EDX, and XRD. Specimens for SEM were sputter coated with a 100 Å layer of gold palladium and imaged using a scanning electron microscope (Hitachi S-4800, Hitachi, Japan). For investigating the depth of CHA conversion, CHA specimen was embedded in epoxy (EpofixTM, Electron Microscopy Sciences, PA, USA) and cut into 300 μm cross-sectional slides. Line EDX was done on these cross-sections of embedded CHA, and general EDX was done on untreated coral, CHA and Sr-CHA to identify different elements on the surfaces. The compositions of all specimens were further characterized by XRD (Model D/max 2550V, Rigaku, Japan) using CuKa radiation (λ = 1.5406 Å) in step-scan mode ($2\theta = 0.02^\circ$ per step).

2.4. In Vitro Study. MC3T3-E1 (ATCC, VA, USA), a mouse osteoblastic cell line, was used to study the cell proliferation on these scaffolds. The cells were cultured in Minimum Essential Alpha (α-MEM) Medium (without ascorbic acid) supplemented with 10% fetal bovine serum (Biosera, UK), Fungizone (1.0 μg/mL), and 1% penicillin/streptomycin in a 37°C incubator with 95% CO_2. Goniopora was cut into $5 \times 5 \times 5\,mm^3$ scaffold and converted to CHA and Sr-CHA. Cells were seeded by putting the scaffolds in a polypropylene container or centrifuge tube with 1 mL (2×10^5 cells/mL) cell suspension for each scaffold. The container was set on a shaker at 300 rpm for 2 h at room temperature. Scaffolds with cell suspension were then transferred to a 24 multiwell plate, and the plate was put in the incubator with the medium changed every other day. Cell proliferation on the scaffolds was studied using the common cell proliferation MTT (3-(4,5-Dimethylthiazol-2-yl)-2,5-diphenyltetrazolium bromide) assay by measuring the metabolic activity of the cells. Viable cells of CHA and Sr-CHA were studied by MTT assay on days 3 and 5.

2.5. Surgical Procedure. An ovariectomized (OVX) model using Sprague-Dawley rat was adopted to preliminarily investigate the *in vivo* properties of the converted corals. Female Sprague-Dawley rats aged 3 months and weighed about 250 g were included. All rats were operated under general anesthesia with 10% ketamine (67 mg/kg) and 2% xylazine (6 mg/kg) (Alfasan, Holland). Bilateral ovariectomy was performed on these rats. Three months after ovariectomy, each of these OVX rats was randomly arranged to receive untreated coral, CHA, or Sr-CHA implants in a disc shape of 3 mm diameter and 2 mm height. A 3 mm diameter bone defect was created on the tibial shaft at about 5 mm below tibia plateau and randomly inserted with implants on both

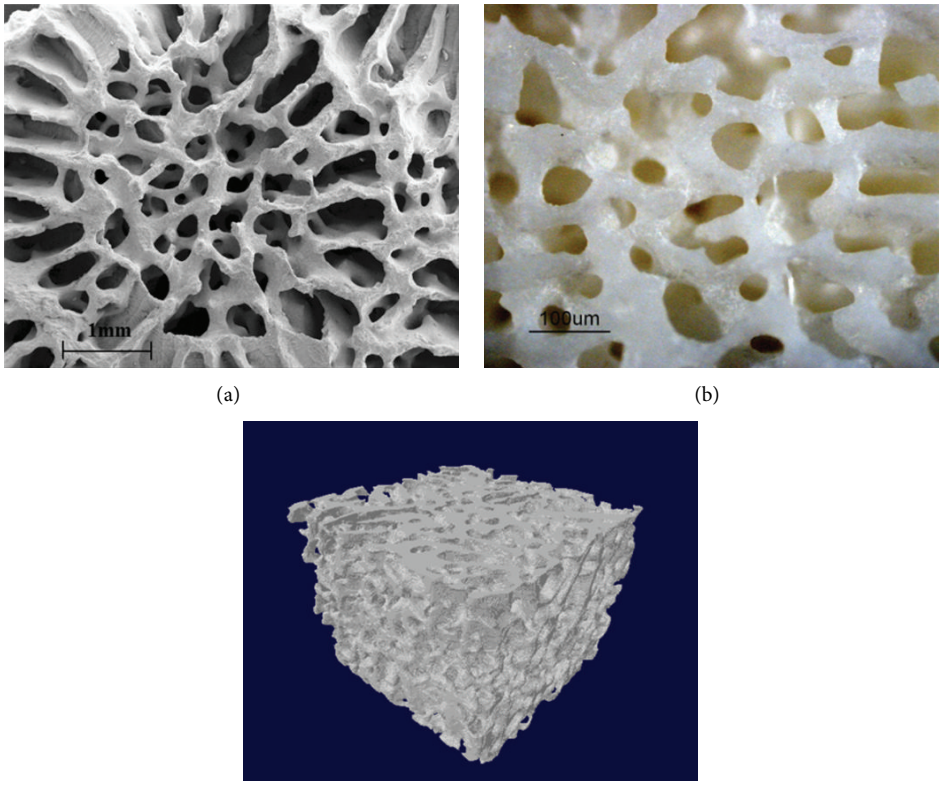

(a) (b)

(c)

Figure 1: (a) Macrostructure of Goniopora captured using SEM at 60x, (b) optical microscope at 100x and (c) 3D micro-CT images.

legs. The wound was closed and wrapped with dressing after implantation.

2.6. Micro-CT Evaluation. Under general anesthesia, these OVX rats were taken for micro-CT scanning on week 0, 1, 2, and 4 after the surgery to evaluate the repairing process of the bone defects and degradation of implants. The images were taken through 180° rotation at a rotation step of 0.60° with the source voltage 88 kV, source current 100 μA, and exposure time of 560 ms. The scaffold volume was processed by SkyScan CTAn and CTvox softwares.

2.7. Statistical Analysis. The results presented in this study are expressed as mean ± standard deviation ($n = 5$ unless specified). Analysis of variance (ANOVA) was applied to calculate the significance level of all data. Statistically significant differences were considered as $P \leq 0.05$; Tukey's post-hoc test was used to study the correlation if statistical significance was obtained.

3. Results

3.1. Macrostructure, 3D Image, and Porosity Measurement. The macrostructure of Goniopora was imaged with an optical microscope (Eclipse 80i, Nikon, Japan), SEM, and micro-CT scanning (as shown in Figure 1). Pore size and thickness of the skeleton can be clearly observed from the optical microscopy and SEM images. The pores are irregular in shape with the majority of the pores having pore sizes between 40–300 μm. Other than the pore size, the thickness of the skeleton is also an important factor determining the porosity; the skeleton thicknesses of Goniopora could be estimated to be around 20–100 μm. The micro-CT scanning is used to visualize the 3D macrostructure and measure the porosity of Goniopora; the porosity is found to be 68.3 ± 12.3%.

3.2. SEM Scanning, EDX and XRD Analyses. Surface morphology, depth of HA conversion, and composition of the corals were studied by SEM, EDX, and XRD. Line EDX was performed on the epoxy embedded cross-sections of untreated coral and CHA to study the depth of conversion as shown in Figures 2(a)–2(d). The dark grey and light grey areas in the SEM images (Figures 2(a) and 2(c)) represent epoxy and coral, respectively. It can be observed that phosphorus was barely detected in raw coral while it reached about 1.3–4 k in CHA specimen (Figures 2(b) and 2(d)). Moreover, the line EDX result also confirmed the complete conversion of CHA from the surface to the core, which was about 1.5 mm from the surface as shown here, and full thickness of the skeleton with the detection of phosphorus coincided with the calcium detected as seen in Figure 2(d).

Surface morphology of the corals after CHA and Sr-CHA treatments was observed with SEM. Goniopora before any treatment was imaged at various magnification to understand

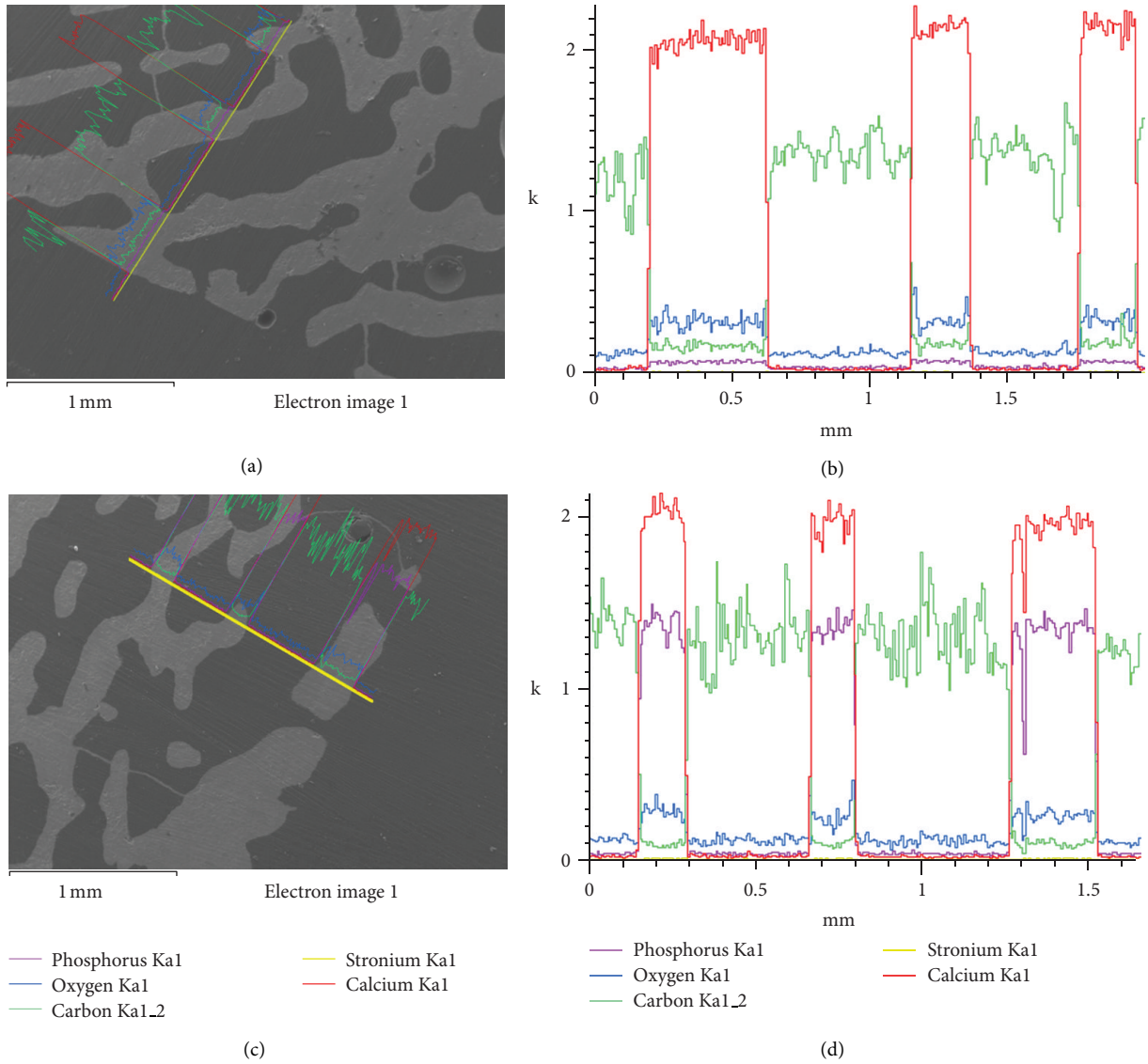

FIGURE 2: Line EDX was performed on untreated coral (a-b) and CHA (c-d) to detect the presences of phosphorus (purple), oxygen (blue), carbon (green), strontium (yellow), and calcium (red).

the microstructure of coral. The skeleton of coral has been reported to be formed by nanofibers and nanograins [19]. As seen in Figure 3(a), the coral was formed by nanograins of diameters <100 nm and nanofibers of diameters 100–500 nm with a few mm in length. After CHA conversion, the surface was covered with flake-like structures (as shown in Figure 3(b)), unlike the surface of raw coral covered with bundles of fibers. A similar structure can be seen in Figures 3(c) and 3(d) after Sr incorporation at different $Sr(NO_3)_2$ concentrations, but the flakes were smaller in size and more spiky in shape for 500 mM $Sr(NO_3)_2$ than 100 mM $Sr(NO_3)_2$. In addition, there were some hexagon rods on the specimens of Sr-CHA, while more and longer rods were found in the 500 mM $Sr(NO_3)_2$ group; these rods were mainly composed of Sr as confirmed by point EDX as Figure 4.

Degree of CHA conversion and percentage of Sr incorporation were carried out by EDX analysis. The elements detected are shown in Figure 5, while the ratio of Ca + Sr/P and percentage of Sr incorporation calculated using EDX data are shown in Table 1. Before hydrothermal conversion, it can be seen that P and Sr were barely detected in the untreated coral. However, the peak of P increases significantly after CHA conversion. The signal of Sr peak becomes distinguishable after Sr incorporation treatment. The Ca + Sr/P calculated on all 3 groups of CHA and Sr-CHA are 1.55 and 1.60, which are lower than the stoichiometric HA of 1.67. Regarding the detection of Sr, 0.8–1.28% of Sr was present in untreated coral and CHA before Sr incorporation; while about 5.94% Sr was detected with less concentrated Sr solution (100 mM $Sr(NO_3)_2$), and 13.78% Sr was detected with more concentrated Sr solution (500 mM $Sr(NO_3)_2$).

The XRD of untreated coral, CHA, and Sr-CHA conversions are shown in Figure 6. The differences between these two treatments on coral can be clearly identified with their

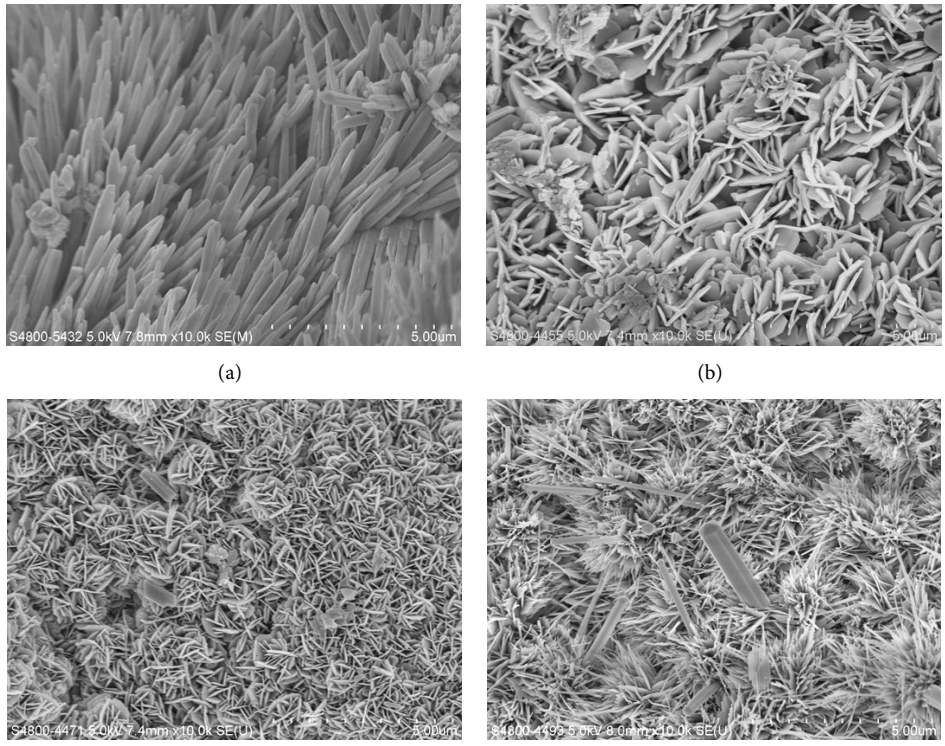

Figure 3: SEM images of: (a) untreated coral, (b) CHA, corals with Sr incorporation in (c) 100 mM, and (d) 500 mM $Sr(NO_3)_2$ solutions.

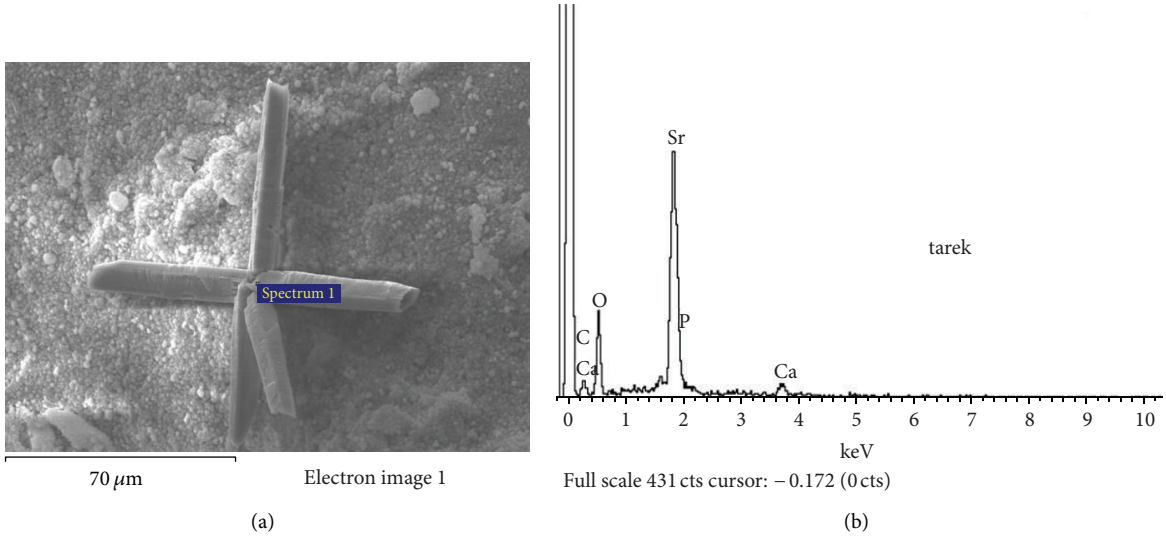

Figure 4: Point EDX was done on a structure formed by hexagonal rods after CHA conversion with Sr incorporation.

Table 1: Ratio of Ca + Sr/P and percentage of Sr incorporated after CHA conversion calculated by EDX analysis.

	Ca + Sr/P mean	SD	Sr/Ca + Sr mean	SD
Untreated	N/A		0.80%	0.19%
CHA	1.55	0.15	1.28%	0.05%
CHA-100 mM Sr	1.55	0.02	5.94%	0.21%
CHA-500 mM Sr	1.60	0.04	13.78%	0.40%

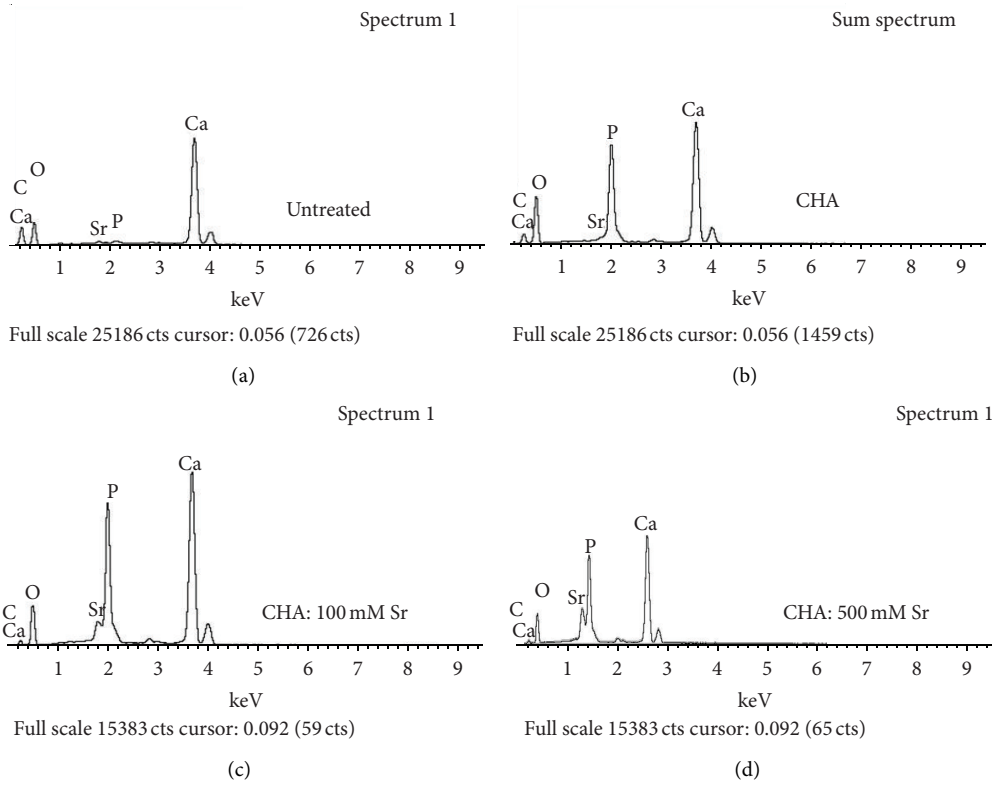

Figure 5: EDX microanalysis spectra of untreated coral, CHA, and Sr-CHA.

Table 2: Measurements of compressive strength and porosity of untreated Goniopora comparing to allogenic cancellous bone, HA, or other bioactive glasses in the literature.

Scaffold materials	Compressive strength (MPa)	Porosity (%)
Goniopora	4.6 ± 0.37	68.3 ± 12.3
Sr-Ca_2ZnSiO_7 [12]	2.16 ± 0.52	78
Ca_2ZnSiO_7 [12]	1.99 ± 0.45	77.5
$CaSiO_3$ [13]	0.32 ± 0.11	81
HA [14]	0.03–0.29	69–86
45S5 Bioglass [15]	0.42–0.60	84–89
Cancellous bone [16–18]	2–9	70–75

different XRD patterns. The XRD patterns of the untreated coral have peaks at 26-27°, 34°, 36–38°, 46–48°, and 50°. However, CHA with and without Sr incorporation obtain different peaks comparing to untreated coral. The identifiable peaks of CHA and Sr-CHA are at 26°, 32–34°, 40°, and 46–54°. The XRD signal at 40° of CHA-500 mM Sr is obviously higher than the signals of CHA-100 mM Sr and CHA.

3.3. Compressive Properties. The compressive strengths after HA conversion with and without Sr incorporation on Goniopora were not compromised or enhanced. Conversion of CHA was performed with 2-3 days of hydrothermal treatments, in which the high temperature and pressure reaction did not seem to affect the mechanical properties of Goniopora. Moreover, CHA conversion and Sr incorporation basically altered the chemical compositions of the coral resulted in changes of the physical structures. The compressive strengths of untreated coral, CHA, and Sr-incorporated CHA with 100 mM and 500 mM $Sr(NO_3)_2$ solutions are in the range of 3.8 to 4.6 MPa as shown in Figure 7. However, no statistical difference is found between all these groups. The compressive strength and porosity of untreated Goniopora were compared to allogenic cancellous bone and scaffolds made of HA or other bioactive glasses as shown in Table 2.

3.4. Cell Culture and Proliferation. In vitro properties of CHA and Sr-CHA (100 mM and 500 mM $Sr(NO_3)_2$) were studied by MTT assay on days 3 and day 5 as shown in Figure 8. On day 3, an estimate of 100,000–140,000 cells was calculated with the greatest number found on CHA; statistical differences were found in CHA comparing to 100 mM and 500 mM $Sr(NO_3)_2$ Sr-CHA. The number of cells increased

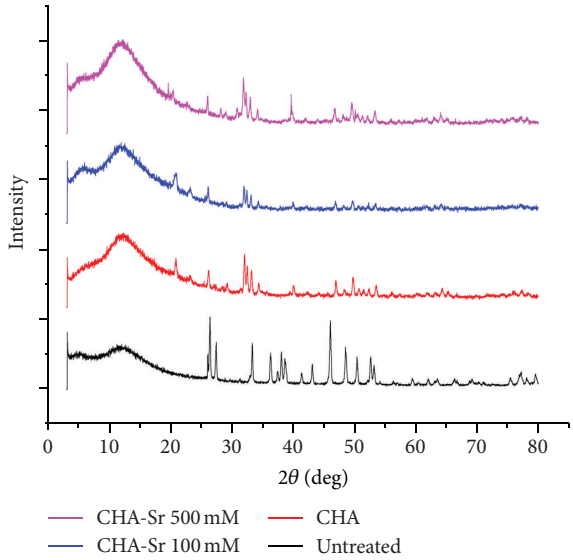

Figure 6: XRD patterns of untreated coral, CHA and Sr-CHA.

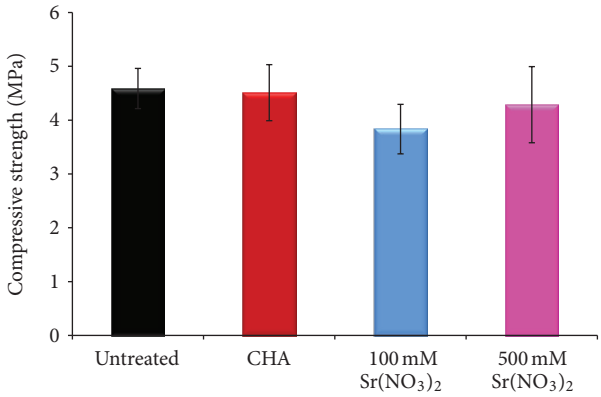

Figure 7: Compressive strengths of untreated coral, CHA, Sr incorporated CHA with 100 mM and 500 mM $Sr(NO_3)_2$ solutions.

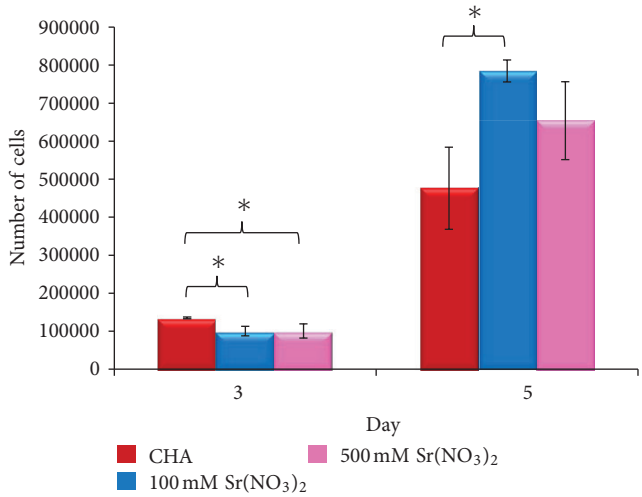

Figure 8: The number of MC3T3-E1 cells on CHA and Sr-CHA on day 3 and 5 with initial seeding of 100,000 cells/scaffold measured by MTT assay (*indicates statistically significant difference for $P < 0.05$).

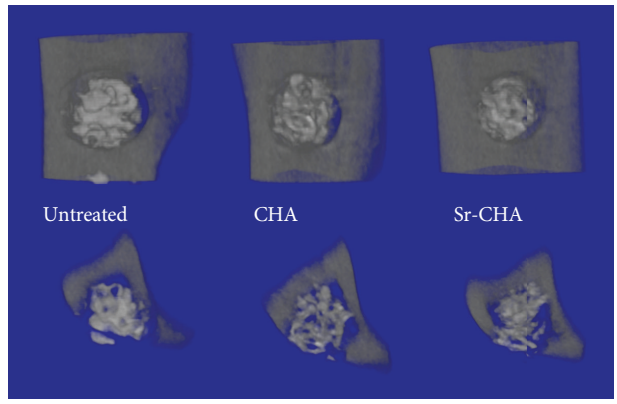

Figure 9: Micro-CT images of the front and cross-sectional views of the untreated coral, CHA, and Sr-CHA at week 2 after implantation.

quite significantly on day 5 in the range of 500,000 to 800,000 cells; CHA was calculated with the smallest number of cells and found to be statistically different from 100 mM $Sr(NO_3)_2$ Sr-CHA. The greatest number of cells is observed with 100 mM $Sr(NO_3)_2$ Sr-CHA specimens.

3.5. Micro-CT Evaluation. The 3D structures of the untreated coral, CHA, and Sr-CHA ($n = 1$) were taken for micro-CT scanning at 0, 1, 2, and 4 weeks after implantation. The micro-CT images of each scaffold taken at the same leg at week 2 are shown in Figure 9, in which the scaffolds can be clearly distinguished from the surrounding cortical bone. All 3 types of scaffolds were undoubtedly degraded in week 4 by a decrease in sizes of the scaffolds and an increase of porosities comparing to week 0. The relative scaffold volumes calculated by the micro-CT results are presented in Figure 10 to give semiquantitative results of the degradation of scaffold or bone growth *in vivo*. There are only about 80% of the volume remained for untreated coral and CHA specimens in the first week after surgery; on the contrary, there are >25% increase in volume, possibility of apatite formation, found in Sr-CHA scaffold. At week 4, more than 50% of the untreated coral and CHA scaffolds degraded, while about 90% of Sr-CHA scaffold remained.

4. Discussion

In this study, Sr was successfully incorporated into coral by hydrothermal conversion. The highly porous structure with interconnectivity of coral has made this naturally occurring material a very attractive material in the area of bone tissue engineering. Over the years, many studies have been done on various genera of corals both in the forms of raw coral or CHA. The interest of Sr in the area of orthopaedic biomaterial flourishes gradually in the last few decades. As a calcium-based material, raw coral, or CHA could be readily incorporated with Sr by simply replacing calcium to a certain

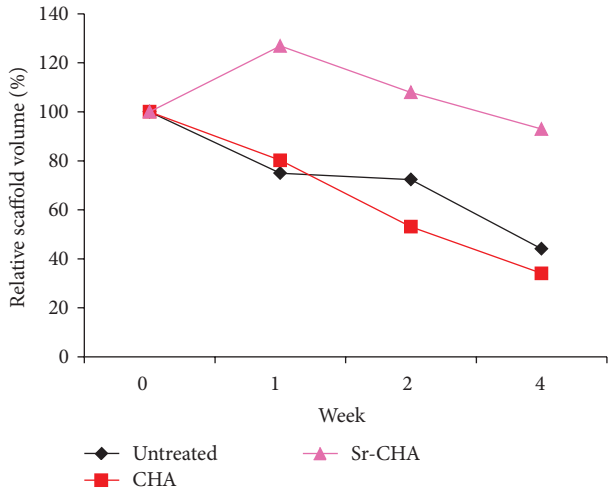

Figure 10: Relative scaffold volumes of different corals at 0, 1, 2, and 4 weeks after implantation calculated by micro-CT results.

extent; the incorporation of Sr should potentially enhance the osteoconductivity or even osteoinductivity of coral as a scaffold.

Like in any orthopaedic biomaterials, interconnected porosity is particularly important in the area of bone tissue engineering because the scaffold is meant to be fully infiltrated with cells as the natural tissue. In addition, porosity is known to be critical in determining the degradation and osteoconductivity of a material [3, 20, 21]. Some of the typical stony corals used as biomaterials are Acropora, Goniopora, and Porties because of the open porosity of their structures. From the porosity measurement measured by micro-CT scanning, Goniopora is found to have a porosity of around 68%. The porosity measurement of Goniopora (~68%) is similar to the results in the literature, in which it is similar to the porosity of cancellous bone [3, 8, 16, 22, 23]. Moreover, the pore sizes and skeleton thicknesses are also critical factors to facilitate the ingrowth of bone or fibrovascular tissue and affect the mechanical properties [3, 4]. The pore sizes of Goniopora are reported in the range of 40–300 μm, which favors the ingrowth of osteoblasts into the scaffold [4, 9].

Hydrothermal conversion of calcium carbonate into CHA with diammonium hydrogen phosphate solution has been frequently performed; however, the degree of conversion was seldom studied since Roy and Linnehan first reported the method in 1974. The standard parameters of hydrothermal treatment were suggested and commonly adopted to be around 180–250°C for 24–48 h [6]. In a previous study of hydrothermally converting conch shell into HA, 2 days and 5 days were proposed in order to convert 120 and 200 μm of calcium carbonate into HA [24]. The thickness of the Goniopora can be seen to be <200 μm from the SEM images, but unlike conch shell, coral is a highly porous structure so that a 2-day and 15 h/day hydrothermal conversion protocol at 180°C was chosen. Line EDX characterization on the cross-sections of embedded CHA confirmed the complete conversion of carbonate by phosphate of this modified protocol.

After HA conversion, there is transformation on the surface morphology compared to untreated coral as imaged by SEM. Over the years, the microstructures of coral have been suggested to be composed of two main structures: center of calcification (COC) (or early mineralization zone) and fibrous zone; structures of nanograins are observed in COC, while nanofibers formed by growth layers of nanograins are found in the surrounding fibrous zone [19, 25–27]. For the untreated Goniopora, nanogranular and nanofibrous structures are clearly observed in the SEM images. Contrastingly, flake-like structures seen in the SEM images of the HA converted corals are the typical surface morphology of CHA [28]. Furthermore, Sr was successfully incorporated into CHA with the presence of hexagon rods after $Sr(NO_3)_2$ treatment, in which the rods were confirmed to be primarily Sr by EDX. However, the percentage of Sr incorporated into CHA was much less than the amount added in the reaction. It indicates the low Sr incorporation efficiency by this current method and the possibility of a limit of Ca replacement in a readily formed microstructure like coral.

A lot of studies applied the hydrothermal reaction to form CHA, but rarely did these studies characterize the Ca to P ratio after conversion. In this study, Ca/P on the specimens after hydrothermal conversion is found to be 1.55 to 1.60. There are two possible explanations for CHA to be in a Ca/P value lower than the stoichiometric value 1.67; calcium-deficient hydroxyapatite (Ca/P = 1.5–1.67) was formed instead of HA or the final product was a mixture of HA and β-TCP. Calcium-deficient HA can be regarded as HA with certain calcium ions replaced by other ions [29]. Although other trace elements are present in corals, which Sr contributed a great percentage and was already taken into the calculation of Ca/P, calcium-deficient HA should not be the form of calcium phosphate in CHA. Xu et al. have suggested that coral was converted to HA via two parallel pathways: (1) direct conversion from aragonite to HA, which starts early during the reaction; (2) from aragonite to calcite, then from calcite to β-TCP, and finally β-TCP conversion to HA [30]. A total of 17 days were required for complete conversion of coral into HA through both pathways mentioned previously. As a result, the calcium phosphate formed after 2 days of hydrothermal reaction in this study should be a mixture of HA and β-TCP but not purely HA.

The XRD patterns of the untreated and HA-converted specimens clearly indicate the change of composition on the surfaces of Goniopora. The untreated Goniopora in this study has the typical peaks of aragonite and looks very much like the XRD pattern of Goniopora reported in the literature [22, 31]. Although 2 small peaks are usually found around 28-29°C on the XRD patterns of HA, there is also a significant peak 29°C reported on calcite [22, 32, 33]. Calcite is a more thermodynamically stable form of calcium carbonate comparing to aragonite [30]. The transformation usually occurs at about 300°C [34, 35]; however, transformation to calcite is proposed to occur as an intermediate process during the hydrothermal conversion of coral aragonite into CHA at temperature <300°C [30]. As a result, it is possible to

detect calcite XRD peak in CHA or Sr-CHA. In general, CHA and Sr-CHA have similar XRD patterns, and all 3 groups have the representable peaks (26°, 32–34°, 40°, and 46–54°) of CHA, which are also the peaks of well-crystallized HA [24, 30, 33, 36, 37]. With the increase of Sr incorporation on synthetic HA particles, the XRD signal at 33-34° should diminish, but it is not the case in this study, while the patterns of CHA and Sr-CHA look almost the same [32]. Only with very high Sr-incorporated HA (40–100%), there should be some shifting of peaks to the left at 28-29° to 27-28° (100% Sr), 32° to 31°, and 33° to 32° [10]. Since only 6–14% of Sr was detected in CHA and Sr-CHA, no apparent signal shift was observed.

Incorporation of Sr altered the chemical composition and surface morphology of CHA, but the compressive strength was neither compromised nor enhanced. The compressive strengths of untreated coral, CHA, and Sr-CHA are in the range of 3.8 to 4.6 MPa, which were greater than the published value (2.62 MPa) for untreated Goniopora or similar to CHA (2.6–4.2 MPa) made with Porites [8, 22, 38, 39]. The porosity and pore size of a material are crucial in determining the mechanical properties, while coral is such an interesting natural material that every single piece is unique; so it is difficult to have exactly the same compressive strength even for the same species of coral. Out of all mechanical properties of orthopaedic biomaterials, compressive strength is a critical factor to look into since our bone is usually under compression. Compressive strength of cancellous bone varied by locations, but in general it is in the range of 2–9 MPa [17, 18, 40]. Based on the compressive strengths of this study, CHA and Sr-CHA converted from Goniopora are advisable for nonload bearing applications.

In order for Sr to have an effect on MC3T3-E1 proliferation, the incorporated Sr should first be able to be released from the scaffold. Sr is undoubtedly added to CHA, but the mechanism of incorporation is still unknown. As it can be seen on the SEM images of Sr-CHA, the Sr in the form of hexagon rod is strongly bounded with the flake-like crystal structures of CHA. The perfect structures of Sr and strong bonding with surface CHA might hinder the release of Sr. Initially, CHA had the greatest number of cells, but the result was reversed at d5, while Sr-CHA had more cells grown. HA conversion and Sr incorporation definitely made changes on the surface chemistry and morphology of coral giving the stimulatory effects of Sr-CHA on MC3T3-E1 cells. The increase of cell number on Sr-CHA indicates the potential of this Sr incorporation approach to enhance osteoblast proliferation on coral, in particular of relatively lower Sr content.

One specimen each of the micro-CT images was analyzed in this current study providing preliminary data of the *in vivo* properties of untreated coral, CHA, and Sr-CHA. Strontium ranelate is a registered medication for treating osteoporosis in many countries, and Sr is also gaining attention to be applied in orthopaedic biomaterials for the last one to two decades. An OVX rat model was chosen in this study to better examine the *in vivo* properties of CHA and Sr-CHA in poor quality bone such as osteoporotic bone in particular. During the period of study, a net volume loss was reported on untreated coral and CHA; more than 50% of the volumes were reduced at week 4 after the surgery. The *in vivo* degradation of a scaffold should be site specific and could vary to a great extent among animals. Natural coral tends to be less favourable than CHA because of the rapid degradation with the scaffold almost completely degraded as early as 4 weeks [41–44]. The loss of volumes of untreated coral and CHA showing the rate of degradation of scaffolds is agreed with the studies in the literature; while HA conversion has no obvious effect on delaying the degradation of coral or promotion of bone formation. On the other hand, there was an increase of the scaffold volume on Sr-CHA 1 week after implantation. This may suggest a net gain of volume resulting from initial apatite formation and minimal scaffold degradation. While untreated coral and CHA degraded pretty quickly, Sr-CHA appeared to induce apatite formation and decelerate the degradation rate with 90% scaffold volume remained at week 4. Formation of apatite layer on the biomaterials has been suggested to induce bone formation [45]; thus, the increase of volume on Sr-CHA due to apatite formation suggests that it favours new bone formation. Unfortunately, it is technically challenging to differentiate apatite or new bone from a radiopaque scaffold primarily based on the micro-CT images. Nonetheless, it is clear that the degradation of Sr-CHA was slower than untreated coral, so this Sr incorporating treatment may be further evaluated to enhance osteoconductivity of coral.

5. Conclusions

A comprehensive study was done to modify and study the mechanical, *in vitro* and *in vivo* properties of Goniopora after HA conversion with Sr incorporation. By characterizing the materials using EDX, SEM, and XRD, the surface morphology and chemical composition were detected with the presence of Sr. It is the first report on incorporating foreign element, Sr in this case, into CHA; it maintains the porous coral structure with the addition of bone stimulating factor Sr. CHA and Sr-CHA were treated to convert the carbonate of Goniopora into phosphate, while the *in vitro* results were encouraging with the possibility of low Sr release. Micro-CT analysis of Sr-CHA has suggested that this Sr-incorporated CHA could enhance bone formation and slow down the degradation of coral. To sum up, this study explored the idea of incorporating Sr into the natural porous structure of coral as potential scaffolding materials.

Conflict of Interests

The authors declare no conflict financial of interests in relation to the work described.

Acknowledgments

This work was funded by Grants from NSFC/RGC (Grant no. N_HKU 739/10), Innovation and Technology Support Programme ITF (GHP/009/06), HKU Seed Funding Programme for Basic Research (no. 201110159010), Natural

Science Foundation of China (Grant no. 81150007), and Shanghai Municipal Education Commission (12YZ039). The authors are grateful for the technical support and guidance from the Electron Microscopy Unit of The University of Hong Kong.

References

[1] H. Burchardt, "The biology of bone graft repair," *Clinical Orthopaedics and Related Research*, vol. 174, pp. 28–42, 1983.

[2] E. M. Younger and M. W. Chapman, "Morbidity at bone graft donor sites," *Journal of Orthopaedic Trauma*, vol. 3, no. 3, pp. 192–195, 1989.

[3] C. Demers, C. Reggie Hamdy, K. Corsi, F. Chellat, M. Tabrizian, and L. Yahia, "Natural coral exoskeleton as a bone graft substitute: a review," *Bio-Medical Materials and Engineering*, vol. 12, no. 1, pp. 15–35, 2002.

[4] B. Ben-Nissan, "Natural bioceramics: from coral to bone and beyond," *Current Opinion in Solid State and Materials Science*, vol. 7, no. 4-5, pp. 283–288, 2003.

[5] M. Cusack and A. Freer, "Biomineralization: elemental and organic influence in carbonate systems," *Chemical Reviews*, vol. 108, no. 11, pp. 4433–4454, 2008.

[6] D. M. Roy and S. K. Linnehan, "Hydroxyapatite formed from coral skeletal carbonate by hydrothermal exchange," *Nature*, vol. 247, no. 5438, pp. 220–222, 1974.

[7] A. J. Ambard and L. Mueninghoff, "Calcium phosphate cement: review of mechanical and biological properties," *Journal of Prosthodontics*, vol. 15, no. 5, pp. 321–328, 2006.

[8] E. C. Shors, "Coralline bone graft substitutes," *Orthopedic Clinics of North America*, vol. 30, no. 4, pp. 599–613, 1999.

[9] S. Yang, K. F. Leong, Z. Du, and C. K. Chua, "The design of scaffolds for use in tissue engineering. Part I. Traditional factors," *Tissue Engineering*, vol. 7, no. 6, pp. 679–689, 2001.

[10] W. Zhang, Y. Shen, H. Pan et al., "Effects of strontium in modified biomaterials," *Acta Biomaterialia*, vol. 7, no. 2, pp. 800–808, 2011.

[11] S.-R. Kim, Y. H. Kim, Y. J. Lee, H.-J. Kim, S.-J. Jung, and H. Song, "Porous hydroxyapatite containing silicon and magnesium, and a preparation method thereof," in *USPO*, Korea Institute of Ceramic Engineering and Technology, Meta Biomed Co. Ltd., Horsham, Pa, USA, 2006.

[12] H. Zreiqat, Y. Ramaswamy, C. Wu et al., "The incorporation of strontium and zinc into a calcium-silicon ceramic for bone tissue engineering," *Biomaterials*, vol. 31, no. 12, pp. 3175–3184, 2010.

[13] C. Wu, Y. Ramaswamy, P. Boughton, and H. Zreiqat, "Improvement of mechanical and biological properties of porous CaSiO3 scaffolds by poly(d,l-lactic acid) modification," *Acta Biomaterialia*, vol. 4, no. 2, pp. 343–353, 2008.

[14] H. W. Kim, J. C. Knowles, and H. E. Kim, "Hydroxyapatite porous scaffold engineered with biological polymer hybrid coating for antibiotic Vancomycin release," *Journal of Materials Science*, vol. 16, no. 3, pp. 189–195, 2005.

[15] Q. Z. Chen, I. D. Thompson, and A. R. Boccaccini, "45S5 Bioglass-derived glass-ceramic scaffolds for bone tissue engineering," *Biomaterials*, vol. 27, no. 11, pp. 2414–2425, 2006.

[16] R. Hodgskinsony, C. Njehz, M. Whiteheadx, and C. Langton, "The non-linear relationship between BUA and porosity in cancellous bone," *hysics in Medicine and Biology*, vol. 41, no. 11, pp. 2411–2420, 1996.

[17] T. M. Keaveny, "Strength of trabecular bone," in *Bone Mechanics Handbook*, S. C. Cowin, Ed., CRC Press, Boca Raton, Fla, USA, 2nd edition, 2001.

[18] J. Rho, "Hard tissues, mechanical properties," in *Encyclopedia of Materials: Science and Technology*, J. K. Buschow, R. W. Cahn, M. C. Flemings, B. Ilschner, E. J. Kramer, S. Mahajan et al., Eds., pp. 3723–3728, Elsevier, Amsterdam, The Netherlands, 2001.

[19] A. Meibom, J. P. Cuif, F. Houlbreque et al., "Compositional variations at ultra-structure length scales in coral skeleton," *Geochimica et Cosmochimica Acta*, 2008.

[20] M. Roudier, C. Bouchon, J. L. Rouvillain et al., "The resorption of bone-implanted corals varies with porosity but also with the host reaction," *Journal of Biomedical Materials Research*, vol. 29, no. 8, pp. 909–915, 1995.

[21] J. E. Davies, "Bone bonding at natural and biomaterial surfaces," *Biomaterials*, vol. 28, no. 34, pp. 5058–5067, 2007.

[22] Y. C. Wu, T. M. Lee, K. H. Chiu, S. Y. Shaw, and C. Y. Yang, "A comparative study of the physical and mechanical properties of three natural corals based on the criteria for bone-tissue engineering scaffolds," *Journal of Materials Science*, vol. 20, no. 6, pp. 1273–1280, 2009.

[23] S. Pollick, E. C. Shors, R. E. Holmes, R. A. Kraut, and J. Glowacki, "Bone formation and implant degradation of coralline porous ceramics placed in bone and ectopic sites," *Journal of Oral and Maxillofacial Surgery*, vol. 53, no. 8, pp. 915–923, 1995.

[24] K. S. Vecchio, "Conversion of sea-shells and other calcite-based materials with dense structures into synthetic materials for implants and other structures and devices," in *USPO*, 2007.

[25] J. P. Cuif and Y. Dauphin, "The Environment Recording Unit in coral skeletons-a synthesis of structural and chemical evidences for a biochemically driven, stepping-growth process in fibres," *Biogeosciences*, vol. 2, no. 1, pp. 61–73, 2005.

[26] J.-P. Cuif and Y. Dauphin, "The two-step mode of growth in the scleractinian coral skeletons from the micrometre to the overall scale," *Journal of Structural Biology*, vol. 150, no. 3, pp. 319–331, 2005.

[27] R. Przeniosło, J. Stolarski, M. Mazur, and M. Brunelli, "Hierarchically structured scleractinian coral biocrystals," *Journal of Structural Biology*, vol. 161, no. 1, pp. 74–82, 2008.

[28] T. Mygind, M. Stiehler, A. Baatrup et al., "Mesenchymal stem cell ingrowth and differentiation on coralline hydroxyapatite scaffolds," *Biomaterials*, vol. 28, no. 6, pp. 1036–1047, 2007.

[29] S. V. Dorozhkin, "Calcium orthophosphates in nature, biology and medicine," *Materials*, vol. 2, no. 2, pp. 399–498, 2009.

[30] Y. Xu, D. Wang, L. Yang, and H. Tang, "Hydrothermal conversion of coral into hydroxyapatite," *Materials Characterization*, vol. 47, no. 2, pp. 83–87, 2001.

[31] J. Hu, R. Fraser, J. Russell, R. Vago, and B. Ben-Nissan, "Australian coral as a biomaterial: characteristics," *Journal of Materials Science & Technology*, vol. 16, no. 2, pp. 591–595, 2000.

[32] Z. Y. Li, W. M. Lam, C. Yang et al., "Chemical composition, crystal size and lattice structural changes after incorporation of strontium into biomimetic apatite," *Biomaterials*, vol. 28, no. 7, pp. 1452–1460, 2007.

[33] B. D. Ratner, A. S. Hoffman, F. J. Schoen, and J. E. Lemons, *Biomaterials Science: An Introduction To Materials in Medicine*, Elsevier, Amsterdam, The Netherlands, 2nd edition, 2004.

[34] S. Yoshioka and Y. Ktiano, "Transformation of aragonite to calcite through heating," *Geochemical Journal*, vol. 19, no. 4, pp. 245–249, 1985.

[35] J. Fricain, R. Bareille, F. Ulysse, B. Dupuy, and J. Amedee, "Evaluation of proliferation and protein expression of human bone marrow cells cultured on coral crystallized in the aragonite of calcite form," *Journal of Biomedical Materials Research A*, vol. 42, no. 1, pp. 96–102, 1998.

[36] J. Hu, J. J. Russell, B. Ben-Nissan, and R. Vago, "Production and analysis of hydroxyapatite from Australian corals via hydrothermal process," *Journal of Materials Science Letters*, vol. 20, no. 1, pp. 85–87, 2001.

[37] R. Murugan and S. Ramakrishna, "Coupling of therapeutic molecules onto surface modified coralline hydroxyapatite," *Biomaterials*, vol. 25, no. 15, pp. 3073–3080, 2004.

[38] R. Holmes, V. Mooney, R. Bucholz, and A. Tencer, "A coralline hydroxyapatite bone graft substitute. Preliminary report," *Clinical Orthopaedics and Related Research*, vol. 188, pp. 252–262, 1984.

[39] J. Vuola, R. Taurio, H. Göransson, and S. Asko-Seljavaara, "Compressive strength of calcium carbonate and hydroxyapatite implants after bone-marrow-induced osteogenesis," *Biomaterials*, vol. 19, no. 1–3, pp. 223–227, 1998.

[40] J. A. Chamberlain, "Mechanical properties of coral skeleton: compressive strength and its adaptive significance," *Palebiology*, vol. 4, no. 4, pp. 419–435, 1978.

[41] M. F. Sciadini, J. M. Dawson, and K. D. Johnson, "Evaluation of bovine-derived bone protein with a natural coral carrier as a bone-graft substitute in a canine segmental defect model," *Journal of Orthopaedic Research*, vol. 15, no. 6, pp. 844–857, 1997.

[42] H. Petite, V. Viateau, W. Bensaïd et al., "Tissue-engineered bone regeneration," *Nature Biotechnology*, vol. 18, no. 9, pp. 959–963, 2000.

[43] F. Geiger, H. Lorenz, W. Xu et al., "VEGF producing bone marrow stromal cells (BMSC) enhance vascularization and resorption of a natural coral bone substitute," *Bone*, vol. 41, no. 4, pp. 516–522, 2007.

[44] Q. Cui, W. M. Mihalko, J. S. Shields, M. Ries, and K. J. Saleh, "Antibiotic-impregnated cement spacers for the treatment of infection associated with total hip or knee arthroplasty," *Journal of Bone and Joint Surgery A*, vol. 89, no. 4, pp. 871–882, 2007.

[45] R. Z. LeGeros, "Properties of osteoconductive biomaterials: calcium phosphates," *Clinical Orthopaedics and Related Research*, no. 395, pp. 81–98, 2002.